

Characteristics of Diluent-Caused Lifted Gas Jet Flames

A. Prasad,* S. Gundavelli,* and S. R. Gollahalli†
University of Oklahoma, Norman, Oklahoma 73019

An experimental study of the liftoff and reattachment characteristics of propane jet flames with addition of nitrogen to the fuel stream at constant jet exit velocity is presented. Flame standoff distance, flame base width, propane mole fraction in the fuel stream at which the transitions occur, radial temperature and concentration profiles in the flame base region, and radiation emission were measured. The results show that flame liftoff exhibits two distinct behaviors when the diluent content of the fuel stream is increased while maintaining the jet exit velocity constant at 6.5 m/s. First, the flame base detaches from the nozzle rim when the propane mole fraction in the jet stream is 0.34 and stabilizes at about 3 nozzle diameters above the nozzle. The flow near the flame base remains laminar. Second, when the propane mole fraction in the jet fluid falls to 0.28 the flame base moves suddenly to a height of about 10 nozzle diameters above the nozzle. The flowfield in the vicinity of the flame base is turbulent in this configuration. The concentration and temperature profiles in the flame base regions of the lifted flames indicate some degree of premixing. Explanations relying on the concept of premixed reactants agree with experimental observations only in the case of the lifted flame with a laminar base and do not account for the stability of the lifted flame with a turbulent base. The trends of the results are consistent with results for the flames with preheated inlet stream and lower jet velocity.

Nomenclature

c	= constant
d	= jet diameter
L	= flame length
l	= macroscale of turbulence
Re_j	= jet Reynolds number at the nozzle exit
Re_λ	= turbulence Reynolds number
r	= radial distance
S_l	= laminar flame velocity
S_t	= turbulent flame velocity
T_j	= temperature at the nozzle exit
\bar{U}	= mean velocity
\bar{u}	= root-mean-square value of the fluctuating velocity
u_j	= velocity at the nozzle exit
u_m	= maximum velocity
w	= flame width
x	= axial distance
x_p	= mole fraction of propane in the jet fluid
λ	= microscale of turbulence
ν	= kinematic viscosity

Introduction

THE stabilization of lifted gas jet flames has received considerable interest in recent years.¹⁻⁷ The mechanism of the stabilization process,^{1,5-7} the structure of the base region,^{2,6} the hysteresis of the reattachment process,^{2,3} and the effect of inlet velocity profile⁴ have been studied. Gas jet flames can be stabilized above the burner by either increasing the exit velocity or diluting the jet fluid.⁸ The latter may occur in burners with exhaust gas recirculation. Earlier studies have focused mostly on flames lifted by high jet velocities. As the jet velocity affects the local flowfield, flame liftoff caused by its increase changes both the flow and the chemical structures of the flame base. Hence, the fluid-dynamic and thermochemical effects cannot be separated. In the present study, flame liftoff was achieved by diluting the inlet fuel stream with an inert gas while keeping the jet exit velocity constant.

Thus, the influence of factors associated with the flowfield is suppressed so that the effects of thermochemical parameters on liftoff process can be assessed. At a certain degree of dilution, the flame detaches from the burner and stabilizes in a region where the local flow is still laminar. However, at a higher degree of dilution, the flame moves to the turbulent region downstream and the liftoff height abruptly increases. Thus, the flame exhibits a two-stage liftoff process. This paper discusses the liftoff characteristics of such flames as well as the structure of the flame base after the transitions.

Experimental Program

The apparatus shown in Fig. 1 consisted of a vertical steel combustion chamber of a square cross section (76 cm × 76 cm × 117 cm). It had air-cooled pyrex glass windows (20 cm × 20 cm × 92 cm) on all four walls. While probing for temperature and concentrations, one of the glass windows was replaced with a slotted metal sheet. After inserting the probe, the slot was sealed with metallic tape. The burner assembly, which was mounted to the floor of the chamber, had a contoured circular nozzle (contraction ratio = 13.5) placed concentrically inside a 162-mm i.d. cylindrical pipe. The nozzle was made of aluminum with inlet and exit diameters of 34.9 mm and 9.5 mm, respectively. The internal

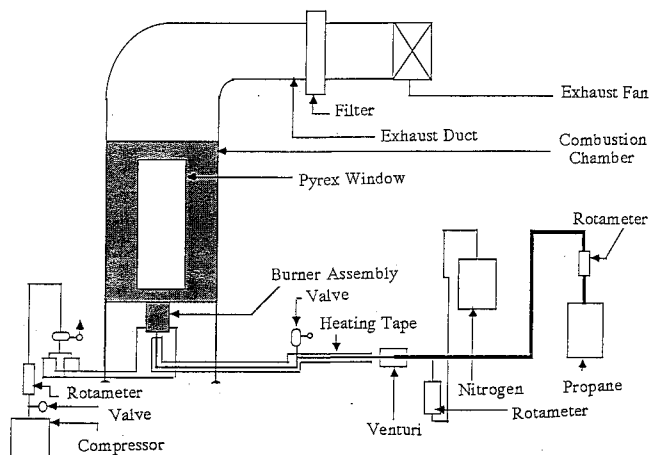


Fig. 1 Schematic diagram of the experimental facility.

Received Jan. 16, 1990; revision received July 17, 1990; accepted for publication Sept. 12, 1990. Copyright © 1990 by the American Institute of Aeronautics and Astronautics, Inc. All rights reserved.

*Graduate Research Assistant, School of Aerospace and Mechanical Engineering.

†Professor, School of Aerospace and Mechanical Engineering.

contour of the nozzle was designed to conform to two tangential circular arcs of diameters 105 mm and 65 mm. Nozzle tips with edges machined to different geometries could be attached to the exit of the convergent section. For the experiments of this study a 9.5-mm i.d. tip with an edge beveled outwards to 60 deg and thickness 0.3 mm was used. The jet fluid was supplied to the nozzle, and combustion air was allowed through the annulus formed by the outer surface of the nozzle and the inner surface of the pipe. Fuel (propane: purity 0.97) and diluent (nitrogen: purity 0.98) were supplied from cylinders, metered with rotameters, and mixed well by flowing them together in a 3-m-long tube leading to the nozzle assembly. Air was supplied from a rotary-vane compressor to the annulus through four diametrically opposite inlets and was passed through a 100-cm-thick honeycomb section and four 200-mesh screens before it entered the combustion chamber. The velocity profile at the exit nozzle tip was flat within 5% of the average value and the mean velocity was held constant at either 6.5 m/s or 5.6 m/s. The secondary air velocity at the exit of the annulus, measured with a hot-wire probe, was also uniform with a mean value of 0.66 m/s. An electronic barocell was used to measure the pressure drop across the nozzle. The velocity calculated from the pressure drop was checked against the average velocities measured with a hot-wire probe and a laser Doppler velocimeter. The combustion chamber was large enough to ensure negligible influence of its walls or the square geometry on the flow in the vicinity of the burner. Further details of the experimental facility are given by Gollahalli et al.⁹

During the liftoff and reattachment studies, the flow rate of propane was changed in increments of a small amount (about 2% of the flow rate of the attached flame) and the flow rate of nitrogen was simultaneously altered to keep the total volume flow rate and hence the exit velocity of the nozzle constant. During the flame-structure measurements, the propane and nitrogen flow rates were kept constant. The secondary airflow rate was also held constant in all of the experiments.

Direct color photography (Kodacolor 100 ASA) was used to determine the flame standoff height (the distance between the nozzle exit and the base of the flame) and width of the flame base. A wide-view angle (150 deg) water-cooled pyrheliometer, mounted on the inside of the chamber wall at half the chamber height, was used to record the incident radiant flux. The temperature field was probed by means of a silica-coated platinum-platinum 13% rhodium (type R) thermocouple with a 0.25-mm bead diameter. The readings were corrected for conduction and radiation losses following Fristrom and Westenberg.¹⁰ Gas samples from the flame base were withdrawn through a cooled stainless-steel probe of tip diameter 1 mm and were treated to remove particulates and water, with a series of line filters and ice-chilled moisture traps. They were analyzed for the concentrations of oxygen, carbon monoxide, and carbon dioxide with nondispersive infrared and polarographic analyzers.

The flowfield in the vicinity of the flame base was probed by means of a laser Doppler velocimeter. This instrument (Aerometrics Phase Doppler Particle Analyzer operated in the LDV mode) was used with a transmitter lens (focal length = 1000 mm), a receiver lens (focal length = 500 mm), and a helium-neon laser (power = 10 mW). The transmitting and receiving optics were mounted on two identical precision traversing mechanisms with a resolution of 80 μ m. The instrument was operated in the forward-scatter mode with a beam separation of 23.8 mm and a beam intersection waist width of 176 μ m. Seeding of the flow was done with a cyclone feeder constructed similar to that described by Glass and Kennedy.¹¹ Both nozzle and coflow streams were seeded with magnesium-oxide particles whose average size was about 5 μ m, chosen for their high melting point close to 2800°C. Seeding of the fuel jet was straightforward. The seeding of coflow, however, posed some difficulties because of the low values of air ve-

Table 1 Experimental conditions

Flame measurement	Propane mole fraction, x_p	Jet velocity, u_j , m/s	Reynolds ^a number
Baseline flame ($T_j = 295^\circ\text{K}$)			
Flame liftoff and reattachment	0.383–0.237	6.5	5410–5160
Temperature and concentration			
Attached	0.383	6.5	5410
Lifted (laminar base)	0.301	6.5	5270
Lifted (turbulent base)	0.243	6.5	5180
Flame radiation	0.383–0.237	6.5	5410–5160
Preheated Inlet Stream ($T_j = 395^\circ\text{K}$)			
Flame liftoff and reattachment	0.383–0.217	6.5	5387–5156
Lower jet velocity ($T_j = 295^\circ\text{K}$)			
Flame liftoff and reattachment	0.383–0.174	5.6	4712–4339

^aBased on the nozzle exit conditions.

locity and agglomeration of particles while passing through honeycombs. A personal-computer data acquisition system with a 16-MHz clock was used to acquire and process the output data of the LDV. The axial mean velocity \bar{U} and the root-mean-square value of the fluctuating components \bar{u} in both the flame and the cold jet were obtained. During measurements in the cold jet, only nitrogen was used as the jet fluid and its flow rate was adjusted to yield the same jet exit Reynolds number as the corresponding flame. As nitrogen was the major component in the jet fluid in flame studies, the cold jet simulation using pure nitrogen did not cause a significant change in the jet-to-ambient density ratio. An estimation of the mixing rates using the relation given by Ricou and Spalding¹² showed that the effect due to the change in the jet-to-ambient density ratio was less than 8%. The results of the study by Brown and Roshko¹³ on turbulent mixing layers also show that the density effects are small. In all runs, 8000 validated samples with sampling times less than 2 s were acquired. Some preliminary experiments showed that the measured values of the mean and rms components of the velocity were not sensitive to the sampling rate above 5000 samples per run. Some experiments were repeated 3–5 times to establish repeatability. The typical values of the spread in the data are shown as uncertainty bars on the figures. Table 1 lists the experimental conditions.

Results and Observations

Flame Appearance

As the propane concentration in the inlet stream was gradually reduced and replaced by nitrogen, the flame appearance changed markedly. First, the color of a large part of the base region of the attached flames (Fig. 2a) turned from yellow to blue, the upper parts of the flame became brighter, and the luminosity of the entire flame increased. A dark space with a thickness of the order of 1 mm, in the radial direction, attributed to the quenching of chemical reactions close to the burner rim, was present in this attached flame and appeared to increase slightly with the decrease of propane content. At a propane mole fraction, $x_p = 0.34$, the length of the dark space suddenly increased and the flame detached from the burner rim and stabilized about 2.5 diameters above the nozzle (Fig. 2b). The edges of the flame appeared straight, smooth, and blue for about five diameters above the flame base. These observations are consistent with the results of an earlier flow-visualization study¹⁴ where the local flow was laminar for

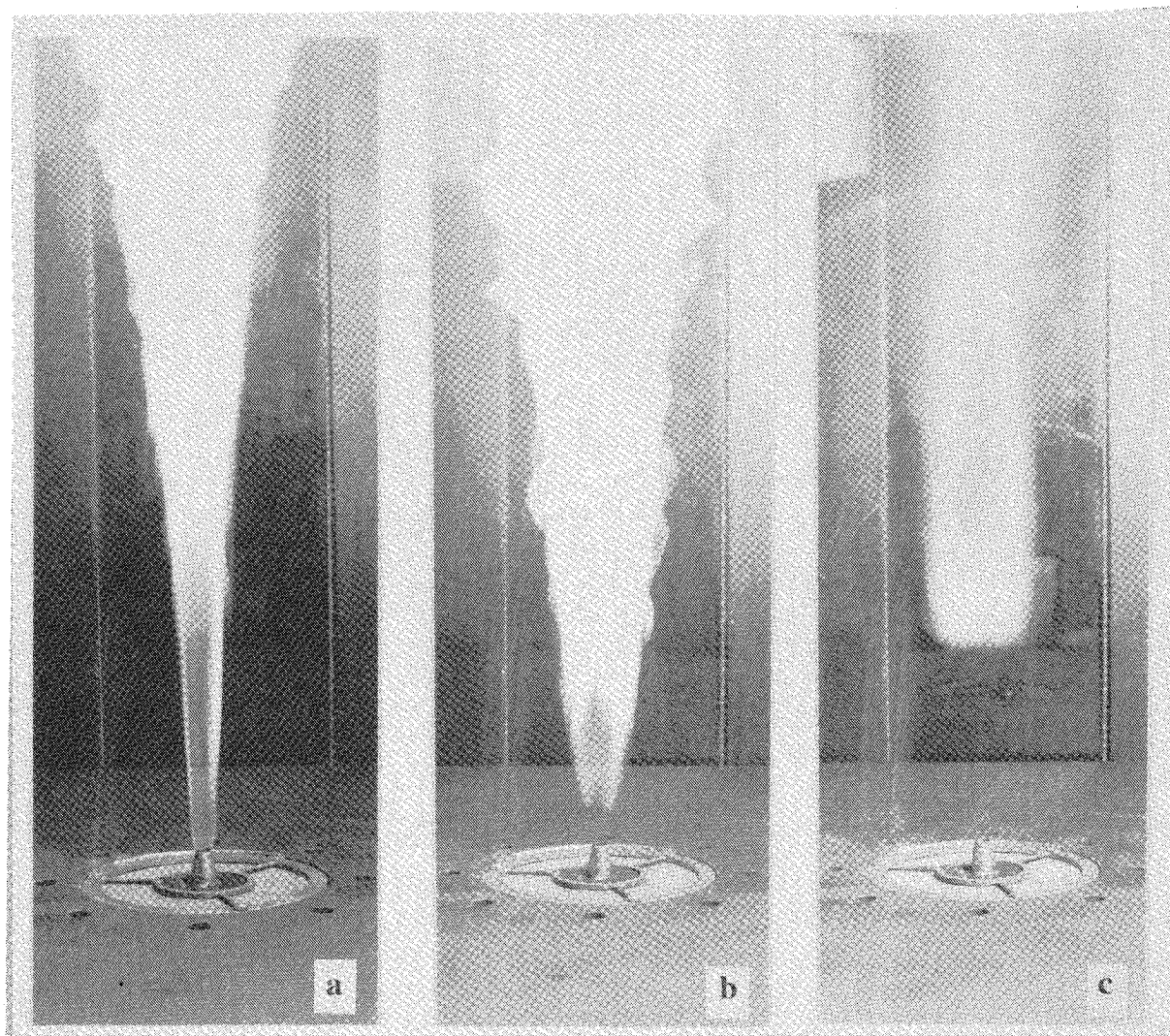


Fig. 2 Photographs of: a) burner-attached flame ($x_p = 0.38$); b) the lifted flame after first transition ($x_p = 0.30$); and c) the lifted flame after second transition ($x_p = 0.24$).

6–8 diameters from the nozzle before the onset of Kelvin-Helmholtz-type instabilities. The flame base was well-defined and sharp for this condition although its position fluctuated less than 2 mm in the axial direction. In this article, the flame after this first transition is called the “lifted flame with laminar base.” When the propane mole-fraction in the jet stream was decreased further, the length of the blue portion gradually increased, and the overall luminosity of the flame decreased. However, the flame-standoff distance changed very little. The flame length was also not markedly different from that before the transition. At $x_p = 0.28$, the flame base jumped suddenly to a height of 10.25 diameters above the nozzle and the width of the flame base also increased substantially (Fig. 2c). The flame-base width at this condition was about twice that of the attached flame at the same distance above the nozzle. The flame base was entirely blue, unsteady, not well-defined, and its position fluctuated over a distance of 15 mm in the axial direction at about 2–4 Hz. Also, azimuthal contortions were evident on the circumference of the flame base. The flame was about 30% shorter than the attached flame. In this paper, the flame after this second transition is called the “lifted flame with turbulent base.” When the propane mole fraction was decreased further, the extent of the blue zone increased, the overall flame length decreased, and the flame-standoff distance gradually increased. At $x_p = 0.23$, the flame appeared highly oscillatory and the position of the flame base fluctuated at 2–3 Hz with an amplitude of 5–8 cm. The flame subsequently extinguished with further decrease of x_p . Thus, the

flame liftoff occurred as a two-stage process in contrast to a single-stage process reported in the studies where liftoff was achieved by only increasing the propane jet velocity.³

Since the position of the flame base after liftoff fluctuated in the streamwise direction, the midpoint of their fluctuation was considered to be the location of the flame base. The temperature and concentration measurements were taken on a time scale larger than 10 s. The flame photography was limited to 1 s to avoid excessive overexposure of the film. Hence, these measurements represent the time-averaged values. As mentioned before, 8000 samples were digitally processed to obtain the mean and rms values of the velocity measurements.

Flame-Standoff Distance and Base Width

Figures 3 and 4 show the variation of dimensionless flame-standoff distance L/d and the width of the flame base w/d measured from photographs exposed for 1 s. The variations of L/d and w/d with decreasing x_p at a constant u_j are similar to their variations with increasing u_j at a constant x_p reported by Gollahalli et al.,³ except that the two-stage process described above is quite evident in the present case.

Also, when propane mole fraction is increased, the reattachment process exhibits a hysteresis similar to that observed when flame liftoff and reattachment were caused by varying the jet velocity.³ The differences in the flow and thermal structures in the upstream parts of the flame base during the

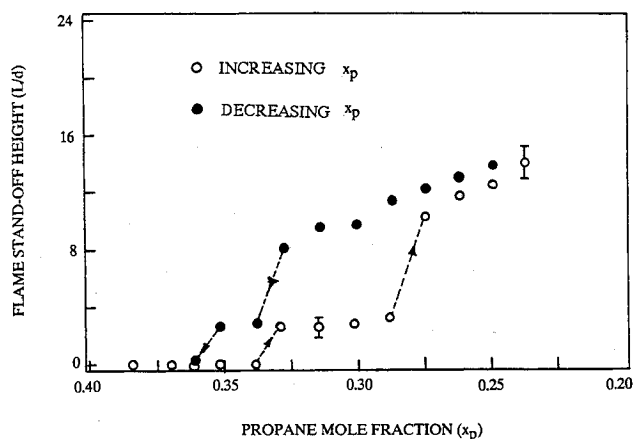


Fig. 3 Variation of flames-standoff height with propane mole fraction in the jet stream.

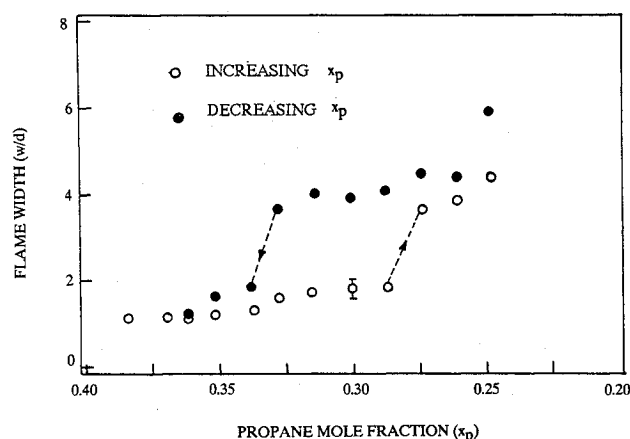


Fig. 4 Variation of flame-base width with propane mole fraction in the jet stream.

lift-off and reattachment processes are probably responsible for the hysteresis in this case also.

Temperature Profiles in the Flame-Base Region

Figure 5 shows the radial temperature profiles in the flame-base region of attached ($x_p = 0.38$) and lifted flames with laminar ($x_p = 0.30$) and turbulent ($x_p = 0.24$) bases. The computed equilibrium adiabatic flame temperatures for the jet fluid combustion in air are 2162°K, 2139°K, and 2112°K, respectively. In all three configurations, the temperature peak value occurs off axis. The location, the value, and the sharpness of the peak confirm the observations described in the previous section. When the first transition occurs, the peak moves radially outward by a small amount and its value increases by about 150°K. The location of the peak corresponds to the measured flame-base width (Fig. 2b). The increase in the value can be attributed to the decrease of continuum radiation indicated by the blue color of the flame base and to the decrease in the conduction heat loss to the nozzle. The changes in the radiation can be traced to the diffusion of surrounding air over the flame-standoff distance as explained later in the section on flame radiation. Since the flowfield is still laminar and the reaction zone is narrow, the peak remains sharp. After the second transition, the flame base is turbulent and its width is greater, as shown by the temperature peak moving considerably further away from the axis. The peak is also much flatter, indicating a more widely distributed reaction zone that can be attributed to the intermittency and the azimuthal contortions. This increased turbulent mixing and higher nitrogen content in the inlet stream decrease the tem-

perature in the flame base. However, the reduction in the continuum radiation, indicated by the intense blue color of the flame base, masks that decrease to some extent. Hence, the peak temperature decreases only slightly.

Concentration Profiles

The radial profiles of carbon dioxide (CO_2) and carbon monoxide (CO) concentrations in the base region of the attached and the two lifted flames are shown in Figs. 6 and 7. These profiles show the same trends as the temperature profiles. The differences between the attached flame and the

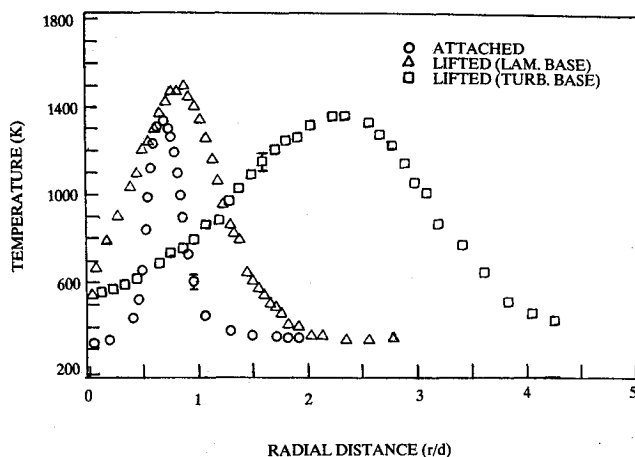


Fig. 5 Radial temperature profiles in the flame, base region of the burner-attached and lifted flames after transition.

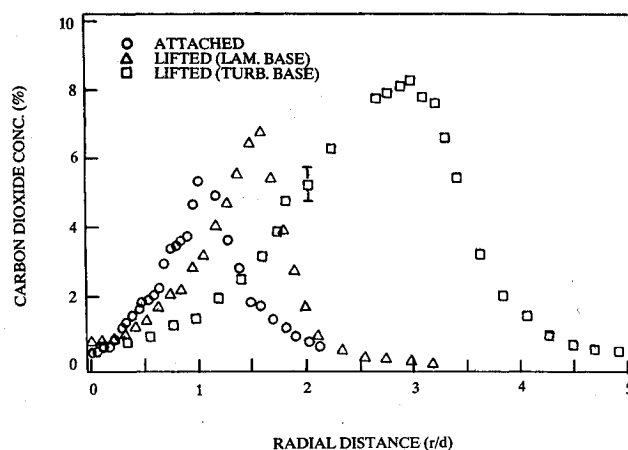


Fig. 6 Radial profiles of carbon dioxide concentration in the base region of the burner-attached and lifted flames after transitions.

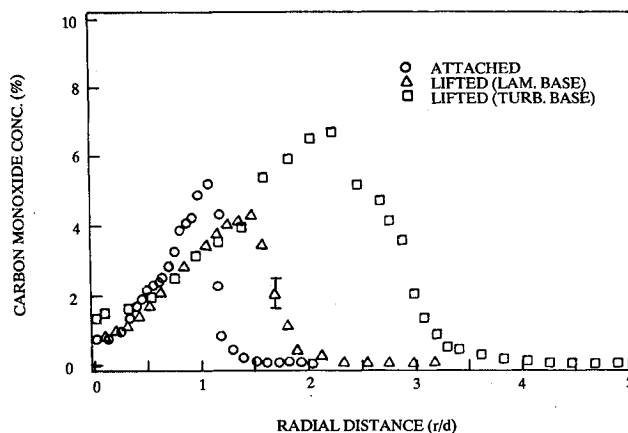


Fig. 7 Radial profiles of carbon monoxide concentration in the base region of the burner-attached and lifted flames after transitions.

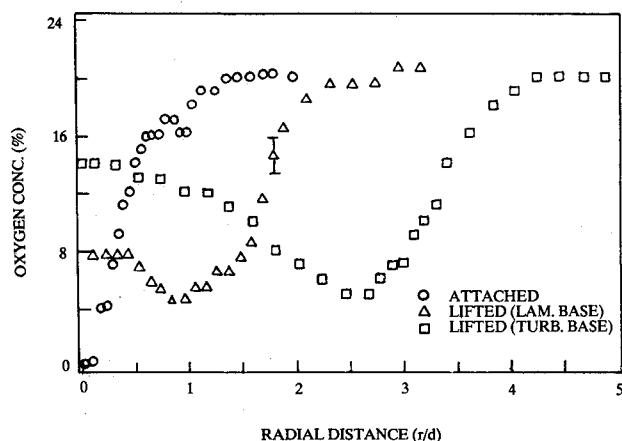


Fig. 8 Radial oxygen concentration profiles in the base region of the burner-attached and lifted flames after transitions.

lifted flame with laminar base are small, whereas the changes are substantial when the flame base becomes turbulent. Note that carbon monoxide concentration peaks occur closer to the axis, i.e., on the fuel side that is characteristic of the dominance of the interface-type reaction. The decrease of CO peak value and the increase of CO₂ peak value in the flame base after the first transition may be attributed to an increase in the rates of fuel pyrolysis and oxidation of lighter fragments to CO₂ by the oxygen (O₂) diffused over the flame-standoff distance. However, both CO and CO₂ peak values increase after the second transition, presumably due to the oxidation of heavier molecules of pyrolyzed fuel with lower hydrogen/carbon (H/C) ratio, and the larger amounts of oxygen diffused over the flame-standoff distance. Hence, these profiles seem to be strongly dependent on the history of the upstream flow. The oxygen concentration profiles shown in Fig. 8 further substantiate the above results. In the attached flame, the oxygen concentration is zero on the axis but in the lifted flame with laminar base it is about 8%. In the attached flame, the O₂ concentration monotonically decreases from the ambient value to zero on the centerline. In the lifted flames, the O₂ concentration on the centerline is higher than that at the locations corresponding to the peak temperature. The higher values on the centerlines of the lifted flames are caused by the diffusion of air over the flame-standoff distance. Also, the concentration gradients show that O₂ enters the reaction zones from both the interior and exterior sides, which explains the enhancement of blue color of the bases of the lifted flames. The differences in the centerline values of O₂ concentration between the two lifted flames can be accounted for by the differences in their flame-standoff distance and the consequent changes in the diffusion time.

Since the hydrocarbon concentrations were not measured in this study and the experiments were limited to the flame base region, the mass balance check of the atomic species was not done.

Flame Radiation

Figure 9 shows the variation of radiation flux incident on a wide-angle radiometer mounted on the combustor wall with the propane mole fraction in the jet stream. This radiometer views the entire flame and has an absorptivity about 0.96 over the wavelength range of thermal radiation. Corrections were made to the readings to remove the contribution of radiation from the chamber walls. The radiation emission from the attached flame increases gradually when the nitrogen content is increased. As the top part of the flame where soot burning dominates is the major contributor to the radiation emission, this increase is in conformity with the visual observations. This increase is primarily attributed to the diffusion of oxygen through the increased thickness of the dark space. Small

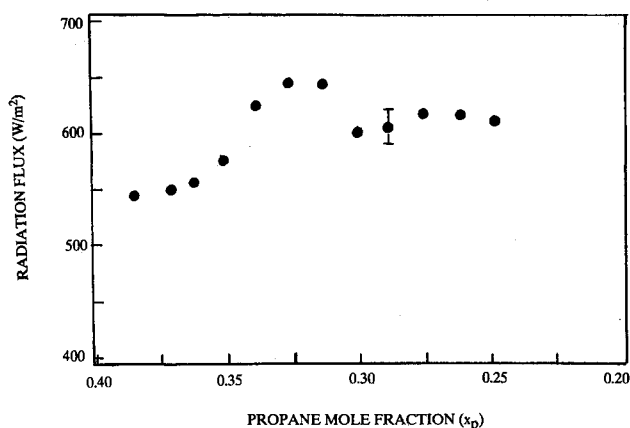


Fig. 9 Radiation emission from the flames after transitions.

amounts of oxygen are known to enhance the pyrolysis and soot formation in diffusion flame.¹⁵⁻¹⁶ Hura and Glassman¹⁷ in their recent study on soot formation in counterflow diffusion burners found that the catalytic effect of oxygen in propane flames is insignificant only at temperatures above 1200°K. Since a substantial part of the propane on the fuel side of the flame exists at temperatures below 1200°K in this study, the catalytic influence of oxygen can contribute to the increase of fuel pyrolysis. The combustion of some of the pyrolysis fragments emits a significant portion of the banded radiation,¹⁸ which explains the enhancement of blue color of the flame base.

After the flame liftoff, a considerably large amount of oxygen is diffused over the flame-standoff distance as noted in the concentration profiles shown in Fig. 8. Then, the influence of oxygen in enhancing the oxidation rates of pyrolysis fragments begins to compete with its effect of increasing soot formation. According to Hura and Glassman,¹⁷ the addition of large amounts of oxygen to the fuel will lead to premixed conditions and result in reduced soot formation, which is evident from the enhanced blue color of the flame base observed in this study. The amount of oxygen mixed with the fuel over the flame-standoff distance and the intensity of blue radiation both are higher in the lifted flame with turbulent base which further supports the above arguments.

Mean and Fluctuating Velocity Profiles

Figures 10-12 show the radial variations of the mean and fluctuating components of axial velocity in the stabilization regions of attached and lifted flames. Also, these figures show corresponding profiles at the same locations for the cold jets. The locations of the visible flame marked by traversing the laser beam are identified. The velocity profiles in the attached and the lifted flame with laminar base are strikingly similar, which is not surprising in view of the similar flow structure of the flame base in both cases. However, the velocity field in the base region of the lifted flame with turbulent conditions is significantly different from those of the other two. At the nozzle exit, the mean velocity profile in the cold jet is uniform over the cross section, as expected. Some extent of its smoothing is noticed in the presence of the flame. The rms values of the fluctuating velocities attain their maxima near the shear layer. More interestingly, the axial component of the mean velocity drops sharply before the flame region. These trends agree well with the flow-visualization results reported by Savas and Gollahalli,¹⁴ where the schlieren pictures showed that the flame zone is located away from the shear layer. Thus, diffusion seems to be the dominant mode of energy and mass transport in the region between the shear layer and the flame zone. This supports the results of Takahashi et al.⁷ and Gollahalli et al.,³ that the detachment of the flame from the nozzle rim occurs under laminar conditions since Kelvin-Helmholtz-

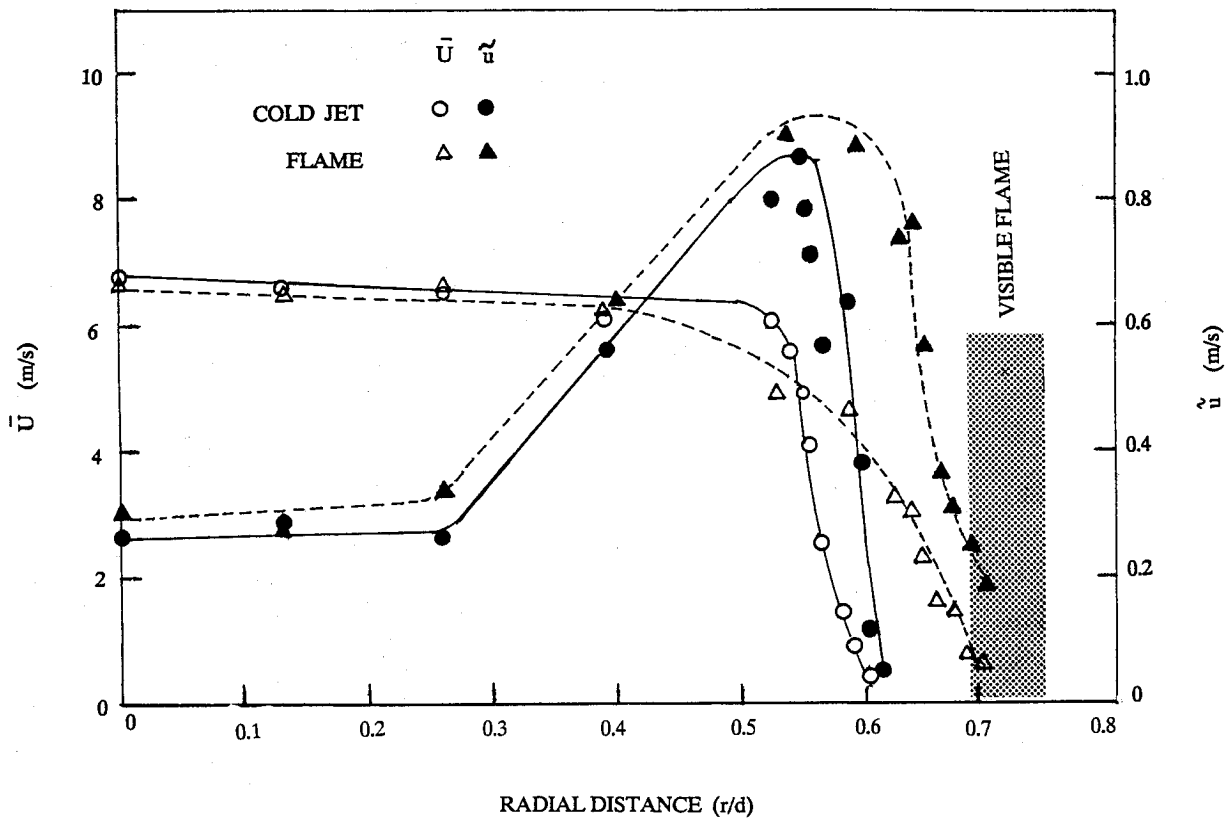


Fig. 10 Mean velocity and turbulence intensities in the base region of the attached flame.

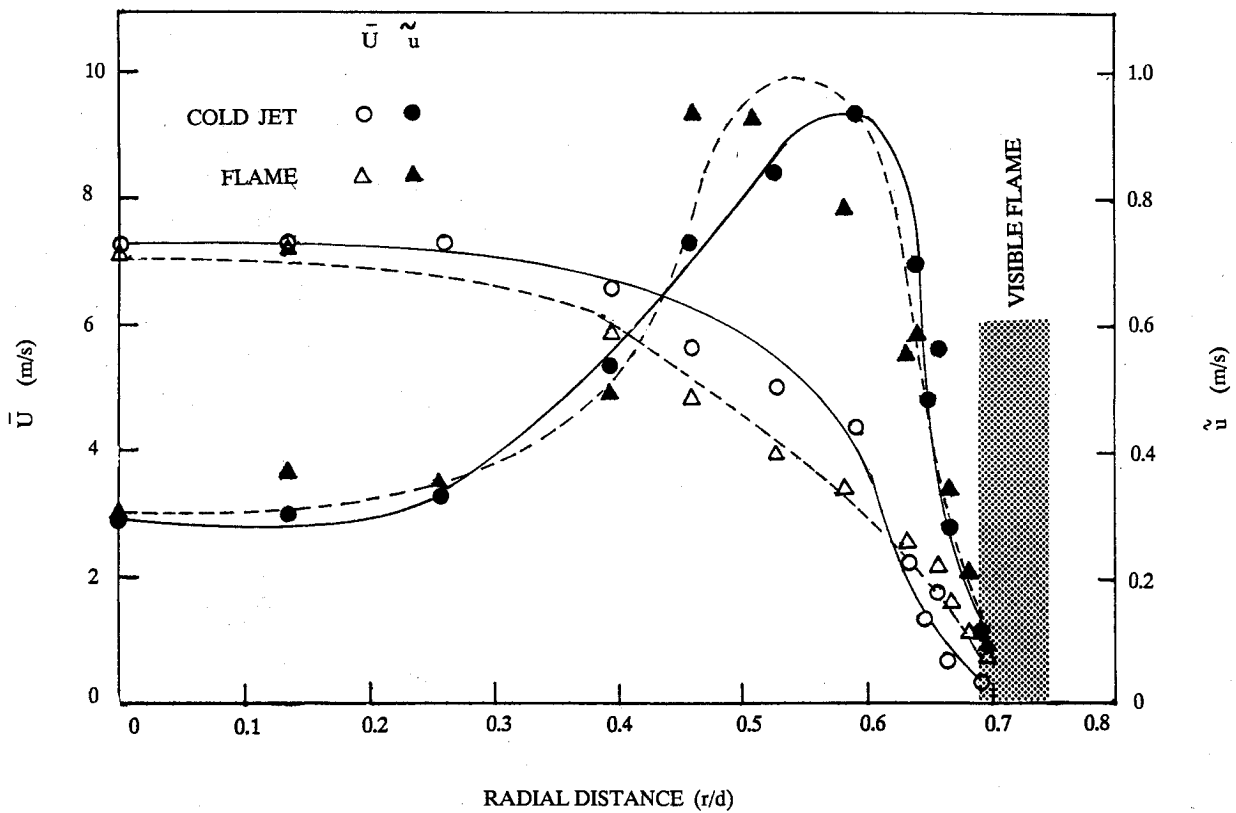


Fig. 11 Mean velocity and turbulence intensities in the stabilization region of the lifted flame with laminar base.

type instabilities develop further downstream. Because of the seeding difficulties, although measurements could not be obtained over the entire flame thickness, the data were obtained close enough to the flame zone to extrapolate them to deduce gas velocities in the flame zone. The profiles reveal that the

magnitudes of the axial velocities are in the range of flame speeds of the jet fluid premixed with air (<0.5 m/s). This implies that although the amount of air diffused is not enough to mix with all of the propane in the jet fluid, it is sufficient to result in a mixture at the edges of the jet, whose flame

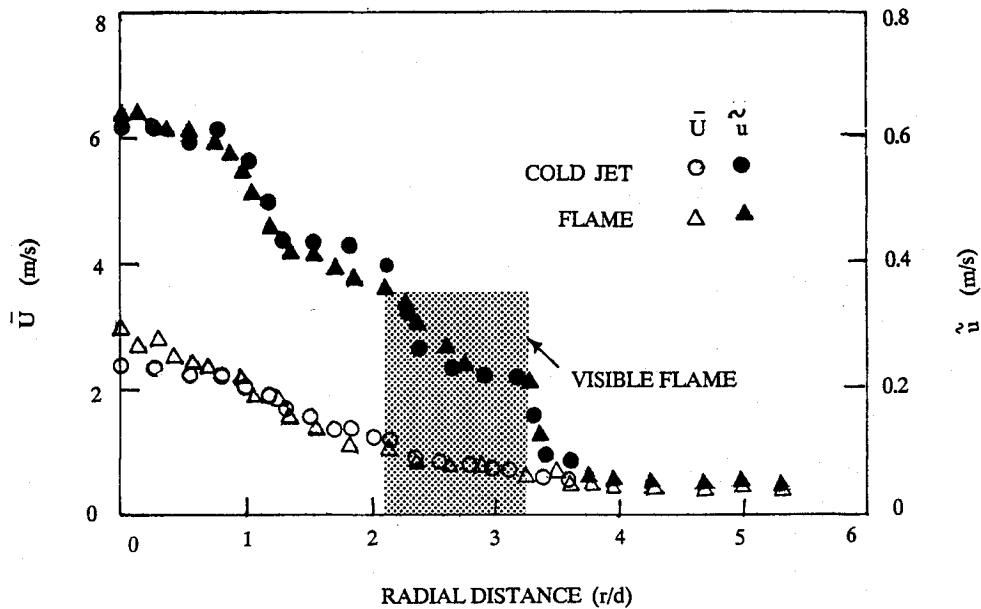


Fig. 12 Mean velocity and turbulence intensities in the stabilization region of the lifted flame with turbulent base.

speed can balance the local gas velocity to keep the flame stable. This is in agreement with the results of Ref. 7.

The root-mean-square value of the fluctuating component of velocity reaches a maximum at about $0.55d$ from the nozzle axis in the attached flame and the corresponding cold jet. That location coincides with the locus of the centers of the large-scale vortices observed in the shear layer.³ This feature is not changed significantly for the lifted flame with laminar base.

Figure 12 shows that in the base of the lifted flame with turbulent conditions both mean velocity and root-mean-square value of the fluctuating component have their peak values on the nozzle axis and decrease monotonically along the radius. The visible flame zone is wider than in the other two cases. The magnitude of the mean velocities in the flame-base region is still about 0.5 m/s and the root-mean-square value of the fluctuations ranges from about 0.4 – 0.2 m/s in the flame zone. Also, in general, the differences in the magnitudes of \bar{U} and \bar{u} at any location in the flame and in its corresponding cold jet are seen to be very small.

Effects of Preheating the Jet Inlet Stream

Some experiments were performed to determine the effect of preheating the inlet stream supplied to the nozzle. Liftoff and reattachment characteristics and flame radiation were measured. The details of those results are available in the report by Gollahalli et al.⁹ The results showed that preheating did not change the general trends. The transitions, from attached to lifted flames with laminar base that subsequently turned turbulent and eventually blew out as the propane concentration is decreased, still occur. The reattachment process also showed hysteresis.³ However, the values of propane concentrations at which the transitions occurred were different.

Table 2 compares the mole fractions of propane at which the transitions occurred, the flame-standoff distance, and the width of the flame base for preheated and unpreheated conditions. The first transition for the preheated condition occurred at a propane mole fraction about 5% lower than for the unpreheated condition. The inlet stream withstood a higher degree of dilution before liftoff when preheated. With preheating of the inlet stream, the laminar flame velocity of propagation increases and hence a higher degree of dilution is needed to overcome it. The second transition occurred at almost the same propane mole fraction in the jet inlet stream for both preheated and unpreheated conditions.

Also, after the first transition, the liftoff distance L/d decreased and the flame-base width w/d increased slightly with preheating. The greater flame width was probably caused by a higher volume flux at the flame base due to volumetric expansion. That would result in the widening of the radial profile of \bar{U} and a decrease in its value at the flame location. To accommodate that variation, the flame base had to move upstream to a location of matching flow velocity. The values near the second transition, however, were within the range of fluctuations of the flame base.

Effect of Lowering Jet Velocity

A further check on the above results was made by performing some experiments with a lower jet velocity while taking care to see that the flow structure at the jet exit was not markedly altered. In this series of experiments, the jet velocity was 5.6 m/s, about 15% lower than the baseline value. The general trends of the flame-liftoff characteristics were the same as those for the other two cases presented above. The values of the propane mole fraction, the flame-standoff distance, and the flame-base width near the transition points are

Table 2 Values of propane mole fraction, flame-standoff distance, and flame-base width at transition points

Jet condition	Lifted flame with laminar base			Lifted flame with turbulent base		
	x_p	L/d	w/d	x_p	L/d	w/d
$u_j = 6.5$ m/s $T_j = 295^\circ\text{K}$	0.337	2.70	1.62	0.275	10.25	3.60
$u_j = 6.5$ m/s $T_j = 395^\circ\text{K}$	0.316	2.40	1.89	0.279	9.44	4.46
$u_j = 5.6$ m/s $T_j = 295^\circ\text{K}$	0.316	2.30	2.10	0.196	12.81	4.93

included in Table 2. In this case also, the values after the first transition varied in the same way as with preheating. The lower jet velocity moved the flame upstream, lowered the flame-standoff distance, and increased the flame-base width. These changes thus are in conformity with the above presented explanations. The flame-standoff distance and the flame-base width near the second transition were, however, fluctuated over approximately the same range as in the experiments with higher jet velocity.

Discussion

In the earlier studies, where the flame detachment from the burner was caused by increasing the jet velocity,^{3,7} the flame liftoff was shown to be a laminar flow phenomenon. It was considered to be governed by the imbalance of the local flow velocity and the maximum flame-propagation velocity of the mixture of jet and external fluids. In the present experiments, as the propane mole fraction in the jet fluid decreases the combustion temperature and laminar flame velocity of the jet fluid-air mixture decrease. When the matching of flow velocity at the nozzle rim, which was kept constant in this study, and the flame velocity cannot occur, the flame moves to a downstream radial location where a lower flow velocity matches the flame velocity. That leads to the first transition. The flame stabilizes at a location where the instabilities are still not developed in the shear layer³ and the mixing is controlled by molecular diffusion. The substitution of nitrogen for propane increases the kinematic viscosity of the jet fluid, decreases the jet exit Reynolds number Re_j , and delays the development of instabilities in the shear layer. As the flow velocity in a cylindrical laminar jet is given by $u_m/u_j = c(Re_d/x)$, where c is a constant, x is axial distance from the nozzle, and u_m is the maximum axial velocity, the local flow velocity decreases.¹⁹ Also, the decrease of propane content of the jet fluid progressively decreases the flame velocity of its mixture with air. Thus, both burning velocity and the local flow velocity decrease, although at different rates, with the substitution of nitrogen in the jet fluid. Consequently, the flame-standoff distance increases slowly with the decrease of propane content for this flame configuration. As the flame velocity is more sensitive than the local flow velocity to the propane concentration, below a certain value of x_p the matching between them fails. However, another matching point downstream is possible when 1) the flame velocity of propagation increases or 2) the combustion occurs in localized stoichiometric zones such as an ensemble of the so-called laminar flamelets. The first situation is possible when the flame velocity of propagation increases because of turbulence and matches the local gas velocity. To check this possibility, the turbulent flame velocity was estimated following the correlation of the ratio of turbulent-to-laminar flame velocity with the turbulence Reynolds number Re_λ based on the macroscale of turbulence given by Andrews et al.²⁰ The turbulence Reynolds number Re_λ was calculated from the relation $Re_\lambda = \bar{u}\lambda/\nu$, where \bar{u} is the rms value of velocity fluctuations, λ is the macroscale, and ν is the kinematic viscosity of the gas mixture, all obtained at cold flow conditions. Also, the value of λ was calculated using the relation $(\lambda^2/l) = 48.64 \nu/\bar{u}$ quoted by Andrews et al., where l is the macroscale of turbulence. According to these authors, the flame structure in such conditions is compatible with the wrinkled laminar flame description. The value of the macroscale of turbulence was taken from the recent detailed measurements of Sislian et al.²¹ and the viscosity of the gas mixture was calculated using Wilke's formula.¹⁹ The values of Re_λ and S/S_L were estimated to be 90 and 5, respectively. Since the amount of diluent nitrogen introduced with the jet fluid is only a small fraction of the stoichiometric amount of air, the laminar flame velocity is expected to decrease to a value of about 0.40 m/s, yielding a value of turbulent flame-propagation velocity of 2 m/s. However, the measured mean velocity in the flame zone at the base of the lifted flame is only about 0.7 m/s. This shows the

stability of the lifted flame with turbulent base cannot be described in terms of the concept of the balance between the local gas velocity and the premixed flame-propagation velocity.

Conclusions

When the inlet stream is progressively diluted with nitrogen while keeping the exit velocity constant, burner-attached propane gas jet flames exhibit two stages of liftoff. With the first transition, the flame detaches from the burner rim and stabilizes within 2–3 diameters above the nozzle. The flow in the base of the flame and its vicinity remains laminar. The second transition is accompanied by a sudden increase in both flame-standoff distance and width of the flame base to much higher values. Also, the flow near the flame base becomes turbulent. The temperature and concentration measurements in the flame base at different configurations show that some amount of premixing of fuel and oxygen occurs upstream of the flame base. The flame-liftoff behavior, however, can be explained in terms of the balance between the local gas velocity and the flame velocity of propagation of the jet fluid and the ambient stream only in the case of the first transition. Estimates of the flame-propagation velocity and the laser velocimeter measurements do not account for the turbulent lifted gas jet flame stability in terms of the concept of premixed reactants at the flame base. The measurements in the flames with preheated inlet stream and lower jet velocity are in conformity with these explanations.

Acknowledgments

The authors thank the U.S. Department of Energy and the Oklahoma Mining and Minerals Resources Research Institute for the funding of this project. The authors also thank Mr. T. Khanna for his help in velocity measurements.

References

- Pitts, W. M., "Assessment of Theories for the Behavior and Blowout of Lifted Turbulent Jet Diffusion Flames," *Twenty-Second Symposium (International) on Combustion*, The Combustion Inst., Seattle, WA, Aug., 1988, pp. 809–816.
- Eickhoff, H., Lenze, B., and Leuckel, W., "Experimental Investigation on the Stabilization Mechanism of Jet Diffusion Flames," *Twentieth Symposium (International) on Combustion*, The Combustion Inst., Ann Arbor, MI, Aug., 1984, pp. 311–318.
- Gollahalli, S. R., Savas, O., Huang, R., and Rodriguez Azara, J. L., "Structure of Attached and Lifted Gas Jet Flames in Hysteresis Region," *Twenty-First Symposium (International) on Combustion*, The Combustion Inst., Munich, West Germany, Aug., 1986, pp. 1463–1471.
- Shekarchi, S., Savas, O., and Gollahalli, S. R., "Structure of a Split Gas Flame," *Combustion and Flame*, Vol. 73, No. 3, 1988, pp. 221–232.
- Broadwell, J. E., Dahm, W. J. A., and Mungal, M. G., "Blowout of Turbulent Diffusion Flames," *Twentieth Symposium (International) on Combustion*, The Combustion Inst., Ann Arbor, MI, Aug., 1984, pp. 303–310.
- Vanquickenborne, L., and van Tigglen, A., "The Stabilization Mechanism of Lifted Diffusion Flames," *Combustion and Flame*, Vol. 10, No. 1, 1969, pp. 59–69.
- Takahashi, F., Mizomoto, M., Ikai, S., and Futaki, N., "Lifting Mechanism of Free Jet Diffusion Flames," *Twentieth Symposium (International) on Combustion*, The Combustion Inst., Ann Arbor, MI, Aug., 1984, pp. 295–302.
- Gollahalli, S. R., and Zadeh, G. K., "Flame Structure of Attached and Lifted Jet Flames of Low-Calorific-Value Gases," *Energy Sources*, Vol. 8, No. 1, 1985, pp. 43–66.
- Gollahalli, S. R., Prasad, A., and Gundavelli, S., "Combustion of Pulverized Coal Blends," Research Rept. OU-AMNE-88-3; Final Rept. Submitted to the Department of Energy, 1988.
- Fristrom, R. M., and Westenberg, A. A., *Flame Structure*, McGraw-Hill, NY, 1965, pp. 150–152.
- Glass, M., and Kennedy, I. M., "An Improved Seeding Method

for High Temperature Laser Doppler Velocimetry," *Combustion and Flame*, Vol. 29, No. 3, 1977, pp. 333-335.

¹²Ricou, F. P., and Spalding, D. B., "Measurements of Entrainment by Axisymmetrical Turbulent Jets," *Journal of Fluid Mechanics*, Vol. 11, No. 1, 1961, pp. 21-32.

¹³Brown, G., and Roshko, A., "On Density Effects and Large Structure in Turbulent Mixing Layers," *Journal of Fluid Mechanics*, Vol. 64, No. 4, 1974, pp. 775-816.

¹⁴Savas, O., and Gollahalli, S. R., "Flow Structure in Near-Nozzle Region of Gas Jet Flames," *AIAA Journal*, Vol. 24, No. 7, 1986, pp. 1137-1140.

¹⁵Wey, C., Powell, E. A., and Jagoda, J. I., "The Effect on Soot Formation of Oxygen in the Fuel of a Diffusion Flame," *Twentieth Symposium (International) on Combustion*, Ann Arbor, MI, Aug., 1984, pp. 1017-1024.

¹⁶Wright, F. J., "Effect of Oxygen Concentration on the Carbon

Forming Tendencies of Diffusion Flames," *Fuel*, Vol. 53, No. 4, 1974, pp. 232-235.

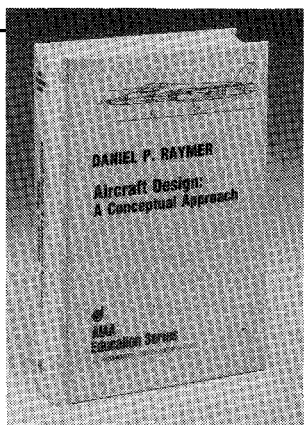
¹⁷Hura, H. S., and Glassman, I., "Fuel Oxygen Effects on Soot Formation in Counter Flow Diffusion Flames," *Combustion Science and Technology*, Vol. 53, No. 1, pp. 1-21.

¹⁸Murray, I., and Sergeant, G. D., "The Onset of Luminosity in Propane/Air Flames," *Fuel*, Vol. 51, No. 4, 1972, pp. 267-271.

¹⁹Kanury, A. M., *Introduction to Combustion Phenomena*, Gordon and Breach Science Publishers, NY, 1977, p. 237.

²⁰Andrews, G. E., Bradley, D., and Lwakabamba, S. B., "Turbulence and Turbulent Flame Propagation—A Critical Appraisal," *Combustion and Flame*, Vol. 24, No. 3, 1975, pp. 285-304.

²¹Sislian, J. P., Jianga, L. Y., and Cusworth, R. A., "Laser Doppler Velocimetry Investigation of the Turbulence Structure of Axisymmetric Diffusion Flames," *Progress in Energy and Combustion Science*, Vol. 14, No. 2, 1988, pp. 99-146.



Aircraft Design: A Conceptual Approach

by Daniel P. Raymer

The first design textbook written to fully expose the advanced student and young engineer to all aspects of aircraft conceptual design as it is actually performed in industry. This book is aimed at those who will design new aircraft concepts and analyze them for performance and sizing.

The reader is exposed to design tasks in the order in which they normally occur during a design project. Equal treatment is given to design layout and design analysis concepts. Two complete examples are included to illustrate design methods: a homebuilt aerobatic design and an advanced single-engine fighter.

To Order, Write, Phone, or FAX:



American Institute of Aeronautics and Astronautics
c/o TASCOT
9 Jay Gould Ct., P.O. Box 753, Waldorf, MD 20604
Phone (301) 645-5643 Dept. 415 FAX (301) 843-0159

AIAA Education Series
1989 729pp. Hardback
ISBN 0-930403-51-7

AIAA Members \$47.95
Nonmembers \$61.95
Order Number: 51-7

Postage and handling \$4.75 for 1-4 books (call for rates for higher quantities). Sales tax: CA residents add 7%, DC residents add 6%. Orders under \$50 must be prepaid. Foreign orders must be prepaid. Please allow 4 weeks for delivery. Prices are subject to change without notice.